Accelerated optical solitons in reorientational media with transverse invariance and longitudinally modulated birefringence

Accelerated optical solitons in reorientational media with transverse invariance and longitudinally modulated birefringence

Urszula A. Laudyn,[1] Michał Kwaśny,[1] Mirosław A. Karpierz,[1] Noel F. Smyth,[2] and Gaetano Assanto[3]

[1] *Faculty of Physics, Warsaw University of Technology, Warsaw 00-662, Poland*
[2] *School of Mathematics, University of Edinburgh, Edinburgh EH9 3FD, Scotland, U.K.*
[3] ***NooEL**— Nonlinear Optics and OptoElectronics Lab*
University of Rome "Roma Tre", 00146 Rome, Italy
and
Photonics Lab, Tampere University of Technology, Tampere FI-33101, Finland

We demonstrate that reorientational spatial solitons can curve when propagating in a medium with engineered walk-off along the direction of propagation. In this regard, we employ nematic liquid crystals with molecular anchoring defined by electron beam lithography and optic axis distribution modulated in the longitudinal direction only, keeping the transverse orientation constant. The experimental results are in remarkably good agreement with a simple modulation theory based on momentum conservation.

PACS numbers: 42.65.Tg, 42.70.Df, 05.45.Yv

I. INTRODUCTION

The unique properties of liquid crystals (LC), combining features of both isotropic liquids and anisotropic crystals, are at the basis of their use in several optical applications [1, 2]. In the absence of absorbing dopants, typical liquid crystalline materials exhibit excellent optical transparency from the ultraviolet to the mid-infrared, high damage threshold and substantial birefringence in the nematic phase, the latter a metaphase with molecules angularly oriented, but positionally disordered [1]. Many practical realizations of LC-based photonic elements and devices have been introduced, including, e.g., displays, gates and routers, optical waveguides, spatial light modulators, variable waveplates and many more [1–4]. All of them benefit from relatively simple and inexpensive fabrication processes, high sensitivity to and tunability with external stimuli, large electro-optic, magneto-optic and nonlinear optical responses. Due to the latter, the last two decades have witnessed extensive efforts towards understanding and exploiting optical spatial solitons in nematic LC (NLC), also termed nematicons [5–7]. Nematicons are two-dimensional, $(2+1)D$ in mathematical terms, optical solitons with stability due to the large nonlocal character of the NLC response caused by intermolecular links in the fluid state [7]. Most NLC are birefringent with positive uniaxiality characterized by refractive indices $n_\parallel$ and $n_\perp < n_\parallel$ for electric fields parallel and perpendicular to the optic axis $\mathbf{n}$, respectively. In NLC, the optic axis coincides with the molecular director, the unit vector describing the average alignment of the elongated molecules. When a light beam with electric field $\mathbf{E}$ propagates in NLC, the induced dipoles undergo a reorientational torque $\Gamma = \epsilon_0 \Delta\epsilon (\mathbf{n}\cdot\mathbf{E})(\mathbf{n}\times\mathbf{E})$, with ϵ_0 the dielectric constant of vacuum and $\Delta\epsilon = n_\parallel^2 - n_\perp^2$. The equilibrium position of the director $\mathbf{n}$ is therefore determined by a balance between the torque and the elastic forces stemming from intermolecular links and anchoring conditions at the boundaries [1, 5, 7]. When the molecular director $\mathbf{n}$ is perpendicular to the electric field, reorientation can only occur above a threshold, the so-called Freedericksz transition [1], which can be avoided by either applying an external voltage to tilt the molecules or by rubbing the cell interfaces and aligning $\mathbf{n}$ at an arbitrary orientation θ_0 in the principal plane defined by $\mathbf{n}$ and the beam wave-vector $\mathbf{k}$. If a finite-size light beam is launched with phasefronts orthogonal to $\mathbf{k}$ as an extraordinary (e) wave with electric field $\mathbf{E}$ coplanar with $\mathbf{n}$ and $\mathbf{k}$, the corresponding refractive index n_e undergoes an increase related to the acquired angular orientation $\theta{=}\theta_0 + \psi$ of $\mathbf{n}$ with respect to $\mathbf{k}$, with ψ the nonlinear optical contribution and $n_e^2(\theta) = n_\perp^2 n_\parallel^2/(n_\parallel^2\cos^2\theta + n_\perp^2\sin^2\theta)$. Thus, self-focusing in reorientational NLC relates to an increase in the extraordinary refractive index due to the reorientation ψ of the optic axis. Moreover, the birefringence of the uniaxial determines the angular departure— the walk-off δ— of the e-wave energy flux— the Poynting vector $\mathbf{S_e}$— from the wave-vector $\mathbf{k}$, with

$$\delta \approx \frac{\Delta\epsilon \sin 2\theta_0}{\Delta\epsilon + 2n_\perp^2 + \Delta\epsilon\cos 2\theta_0} \qquad (1)$$

in the weakly nonlinear regime $|\psi| \ll \theta_0$. Hence, nematicons are reorientational, self-trapped, extraordinarily-polarized wavepackets which propagate rectilinearly in the principal plane with transverse velocity δ with respect to $\mathbf{k}$ [8–10]. Moreover, the light-induced refractive index modulation $n_e(\theta) - n_e(\theta_0)$ gives rise to a graded-index channel waveguide able to confine and route other (weak and co-polarized) optical signals, making nematicons an excellent platform for realizing dynamic (real time) guided-wave circuits for optical processing [11–13] or even permanent ones upon polymerization of the beam-defined structures [14]. In the context just described, it is highly relevant to engineer/control nematicon trajectories and the corresponding waveguide paths by acting on walk-off

and/or phasefront curvature, the two effects being interconnected through their θ-dependence in uniaxial media.

A number of viable approaches have been reported in order to modify nematicon trajectories by altering θ_0, including voltage-driven rotation of the principal plane [9], electro-optic orientation [15–18], refraction and total internal reflection at an NLC-NLC interface [19–22], light-induced director changes in the highly nonlinear regime [23–27], chiral doping [28, 29], magneto-optic orientation [30, 31], etc. Moreover, even in the absence of polarization dynamics giving rise to a Pancharatnam-Berry geometric phase for light propagation in bulk [32, 33], nematicons and their waveguides can be bent by propagating in NLC with a transverse modulation of the optic axis distribution, as we recently predicted and demonstrated [34, 35]. In this Paper we investigate, both theoretically and experimentally, nematicon propagation in non-uniformly aligned NLC with a longitudinally varying, but transversely constant optic-axis orientation, i.e., with $\theta_0 = g(z)$.

At variance with previous investigations and reports, this particular configuration allow us to single out the effects of the birefringent walk-off on the beam trajectory, excluding refraction and phasefront distortions, as the index distribution of the medium remains uniform across the beam profile, with n_e and the effective birefringence $n_e - n_\parallel$ changing in the propagation direction only. This studied case encompasses an input beam with electric field polarized along y and wavevector $\mathbf{k} \parallel \hat{\mathbf{z}}$, a director orientation in the principal plane $\hat{y}\hat{z}$ and a linear variation of θ_0 along $\hat{z}$, with all the parameters constant across the other transverse axis $\hat{x}$ (thickness). The experimental results in planar samples realized by electron-beam lithography are in excellent agreement with a simple model based on modulation theory and momentum conservation, demonstrating the easy design and feasibility of such non-uniform structures for curved and bent all-optical waveguides.

II. SAMPLE GEOMETRY AND EXPERIMENTAL CONFIGURATION

We prepared 30μm-thick NLC samples with in-plane anchoring at the inner interfaces of a planar glass cell, using the mixture 6CHBT (synthesized at the Military University of Technology, Warsaw, Poland [36]) with $n_\perp = 1.4967$ and $n_\parallel = 1.6335$ at room temperature and wavelength $\lambda = 1064nm$, critical temperature $T_c = 43^0C$ and elastic constants $K_{11} = 8.96pN$, $K_{22} = 3.61pN$ and $K_{33} = 9.71pN$ for splay, twist and bend, respectively.

The cell was fabricated with $1.1mm$-thick BK7 glass slides; the propagation length was 1 or 2 mm along z, depending on the geometry. In order to realize the modulated orientation, the upper and lower slides were exposed to electron-beam lithography in order to define the molecular director anchoring θ_0 at the boundaries across the thickness x [35, 37]. The angular modulation was implemented at a $1^0/11\mu$m rate.

Figure 1(a) is a sketch of the sample with uniform distribution $\theta_0 = 45^0$. Such an orientation prevents the Freedericksz transition and maximizes the nonlinear response [38]. We injected a linearly polarized Gaussian beam at $\lambda = 1064nm$ with electric field oscillating along $\hat{y}$, focused by a microscope objective to a waist $w_0 \approx 3\mu$m at the input in order to launch a nematicon. A CCD camera acquired the out-of-plane scattered light and monitored the beam evolution in the plane $\hat{y}\hat{z}$. In this case, the nematicon trajectory is determined only by the constant walk-off, leading to a rectilinear path, as visible in Fig. 1(b). Fig. 1(c) graphs the calculated extraordinary refractive index and walk-off versus the initial (at rest) director alignment θ_0 for this specific NLC. Close to $\theta_0 = 45^0$ the walk-off reaches its maximum of nearly $\delta = 5^0$.

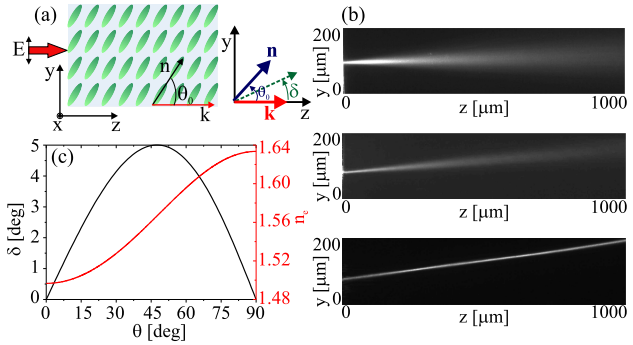

FIG. 1: (a) Sketch of the sample with uniform orientation; (b) acquired images of diffracting ordinary wave beam (top) and extraordinary wave beams featuring linear diffraction at low power (center) or self-confinement at high power (bottom), respectively; (c) calculated walk-off (black line) and extraordinary-wave refractive index $n_e(\theta)$ versus molecular orientation $\theta = \theta_0$ (red line).

Figure 2(a–b) sketches NLC configurations with a linearly modulated angle $\theta_0(z)$ along the longitudinal coordinate z in the principal plane. In Fig. 2(a) the orientation changes continuously from 45^0 to -45^0 and in Fig. 2(b) the angle changes from 45^0 to -45^0 and back to 45^0, over twice the propagation length of the previous structure in Fig. 2(a). The variations in θ_0 affect both the refractive index and the walk-off (Fig. 2(c)) of the extraordinary-wave beam; in addition, the nonlinear response tends to vanish whenever θ_0 approaches zero.

III. MOMENTUM CONSERVATION

The experimental results can be modelled by the propagation of a linearly polarized, extraordinary wave of wavelength λ, wavenumber k_0 and power P_0 through bulk uniaxial NLC with orientation of the optic axis which varies down the cell. The polarization of the electric field $\mathbf{E} = \mathbf{E_y}\hat{\mathbf{y}}$ is taken to be the y direction.The NLC molec-

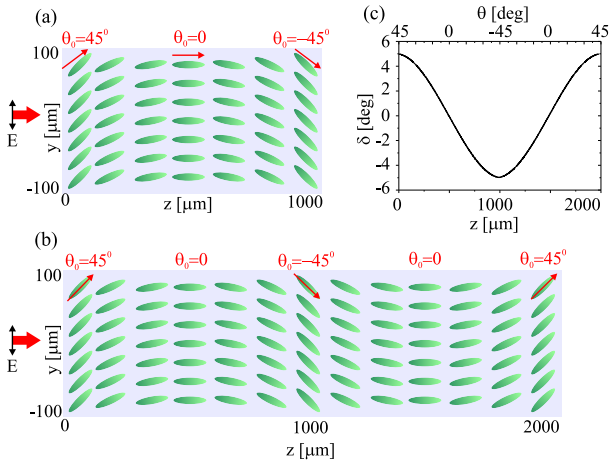

FIG. 2: (a) Sketch of a cell with linearly changing molecular orientation along the propagation direction z from 45^0 via 0^0 to -45^0; (b) sketch of a cell with doubly linear modulation from 45^0 to -45^0 and back to 45^0; (c) calculated walk-off versus θ_0 and z for the case (b).

ular director rotates in the (y,z) plane, with its orientation θ measured from $\mathbf{k} \parallel \hat{\mathbf{z}}$. The light beam is input at $y = y_0$ at $z = 0$, at which point the director forms an angle θ_0. The orientation varies with z down the cell with $\theta_0(z) = \theta_0(0) + \theta_b(z)$. Finally, the beam causes an additional all-optical reorientation denoted by ψ. Hence, the total angle of the optic axis with the z direction is $\Phi = \theta_0(0) + \theta_b(z) + \psi(x,y,z)$.

The pointwise extraordinary refractive index n_e is given in terms of the director orientation by

$$n_e^2(\Phi) = \frac{n_\perp^2 n_\parallel^2}{n_\parallel^2 \cos^2\Phi + n_\perp^2 \sin^2\Phi}, \tag{2}$$

where, as defined above, $n_\perp$ and $n_\parallel$ are the refractive index eigenvalues. The optical anisotropy is defined as $\Delta\epsilon = n_\parallel^2 - n_\perp^2$. In the paraxial, slowly varying envelope approximation the equations governing the evolution of the beam in NLC are then [7]

$$\begin{aligned} &2ik_0 n_e \frac{\partial E_y}{\partial z} + 2ik_0 n_e \Delta(\Phi)\frac{\partial E_y}{\partial y} + \nabla^2 E_y \\ &+ k_0^2 \left(n_\perp^2 \cos^2\Phi + n_\parallel^2 \sin^2\Phi \right. \\ &\left. - n_\perp^2 \cos^2\theta_0 - n_\parallel^2 \sin^2\theta_0 \right) E_y = 0, \end{aligned} \tag{3}$$

for the electric field of the light beam and

$$K\nabla^2\Phi + \frac{1}{4}\epsilon_0 \Delta\epsilon |E_y|^2 \sin 2\Phi = 0 \tag{4}$$

for the medium response. In the director equation (4) the single elastic constant approximation has been made so that the elastic constants for bend, twist and splay are taken equal to K. Here, the Laplacian ∇^2 is in the transverse (x,y) plane. The walk-off δ is expressed in terms of the coefficient Δ in the electric field equation (3) by $\tan\delta = \Delta$, with

$$\Delta(\Phi) = \frac{\Delta\epsilon \sin 2\Phi}{\Delta\epsilon + 2n_\perp^2 + \Delta\epsilon\cos 2\Phi} \tag{5}$$

and $\Delta(\Phi) \approx \Delta(\theta_0(z))$ in the weakly nonlinear regime. K is the elastic constant of the NLC in the single constant approximation, assuming equal elastic constants for bend, twist and splay.

In their full form, the nematic equations (3) and (4) are difficult to solve, or even find approximate solutions for. But a low power approximation can be made so that asymptotic solutions can be derived. For low power beams, the optical reorientation ψ is much less than the imposed orientation $\theta_0(0)+\theta_b$, $|\psi| \ll |\theta_0(0)+\theta_b|$. In this case the trigonometric functions in these equations can be expanded in Taylor series about $\theta_0(0)+\theta_b$. In this low power limit, equations (3) and (4) become

$$\begin{aligned} &2ik_0 n_e \frac{\partial E_y}{\partial z} + 2ik_0 n_e \Delta(\theta_0(0)+\theta_b)\frac{\partial E_y}{\partial y} + \nabla^2 E_y \\ &+ k_0^2 n_\perp^2 \left[\cos^2(\theta_0(0)+\theta_b) - \cos^2\theta_0(0)\right] E_y \\ &+ k_0^2 n_\parallel^2 \left[\sin^2(\theta_0(0)+\theta_b) - \sin^2\theta_0(0)\right] E_y \\ &+ k_0^2 \Delta\epsilon \sin 2(\theta_0(0)+\theta_b)\,\psi E_y = 0, \end{aligned} \tag{6}$$

$$K\nabla^2\psi + \frac{1}{4}\epsilon_0\Delta\epsilon |E_y|^2 \sin 2(\theta_0(0)+\theta_b) = 0. \tag{7}$$

The electric field equation (6) can be simplified using the phase transformation

$$\begin{aligned} &E_y = \tilde{E}_y \times \\ &\exp\left(\frac{ik_0}{2n_e} \int_0^z \left[n_\perp^2 \left(\cos^2(\theta_0(0)+\theta_b(z)) - \cos^2\theta_0(0) \right) \right.\right. \\ &\left.\left. + \; n_\parallel^2 \left(\sin^2(\theta_0(0)+\theta_b(z)) - \sin^2\theta_0(0) \right) \right] dz \right). \end{aligned} \tag{8}$$

After this transformation, the nematic equations become

$$\begin{aligned} &2ik_0 n_e \frac{\partial \tilde{E}_y}{\partial z} + 2ik_0 n_e \Delta(\theta_0(0)+\theta_b(z))\frac{\partial \tilde{E}_y}{\partial y} + \nabla^2 \tilde{E}_y \\ &+ k_0^2 \Delta\epsilon \sin 2(\theta_0(0)+\theta_b(z))\,\psi \tilde{E}_y = 0, \end{aligned} \tag{9}$$

$$K\nabla^2\psi + \frac{1}{4}\epsilon_0\Delta\epsilon |\tilde{E}_y|^2 \sin 2(\theta_0(0)+\theta_b(z)) = 0. \tag{10}$$

The final simplification is obtained by setting the equations in non-dimensional form. We define the scalings W for the transverse directions, D for the longitudinal direction and E for the electric field as

$$x = WX, \quad y = WY, \quad z = DZ, \quad \tilde{E}_y = Eu. \tag{11}$$

Let us take the input beam to be a Gaussian beam of power P_0 and width W_b. It is then found from equations (9) and (10) that suitable scaling parameters are

$$\begin{aligned} &W = \frac{\lambda}{\pi\sqrt{\Delta\epsilon \sin 2\theta_0(0)}}, \quad D = \frac{2n_e\lambda}{\pi\Delta\epsilon \sin 2\theta_0(0)}, \\ &E^2 = \frac{2P_0}{\pi C W_b^2}, \quad C = \frac{1}{2}\epsilon_0 c n_e, \end{aligned} \tag{12}$$

so that the nematic equations (9) and (10) in non-dimensional form are

$$i\frac{\partial u}{\partial Z} + i\gamma\Delta(\theta_0(0)+\theta_b(Z))\frac{\partial u}{\partial Y} + \frac{1}{2}\nabla^2 u + 2\frac{\sin 2\left(\theta_0(0)+\theta_b(Z)\right)}{\sin 2\theta_0(0)}\psi u = 0, \quad (13)$$

$$\nu\nabla^2\psi + 2\frac{\sin 2\left(\theta_0(0)+\theta_b(Z)\right)}{\sin 2\theta_0(0)}|u|^2 = 0, \quad (14)$$

with the Laplacian ∇^2 in the transverse non-dimensional variables (X, Y). The parameters γ and ν are

$$\gamma = \frac{2n_e}{\sqrt{\Delta\epsilon\sin 2\theta_0(0)}} \quad \text{and} \quad \nu = \frac{8K}{\epsilon_0\Delta\epsilon E^2 W^2\sin 2\theta_0(0)}. \quad (15)$$

This non-dimensional form of the model will be used to analyze the trajectory of a nematicon owing to the varying orientation θ_b. In the case of a uniform NLC, so that $\theta_b = 0$, equations (13) and (14) reduce to a standard form [39].

The trajectory of a nematicon in non-uniform NLC can be found using what is mathematically momentum conservation for the solitary wave. The simplest method to find this momentum equation is from the Lagrangian formulation of the nematic equations (13) and (14), which is

$$L = i\left(u^* u_Z - u u_Z^*\right) + i\gamma\Delta(\theta_0(0)+\theta_b(Z))\left(u^* u_Y - u u_Y^*\right) - |\nabla u|^2 + 4\frac{\sin 2\left(\theta_0(0)+\theta_b(Z)\right)}{\sin 2\theta_0(0)}\psi|u|^2 - \nu|\nabla\psi|^2. \quad (16)$$

The * superscript denotes the complex conjugate and the Z and Y subscripts denote derivatives. In principle, the momentum equation for a nematicon is now found by substituting the nematicon solution for u and ψ into the Lagrangian (16). This Lagrangian is then "averaged" by integrating in X and Y from $-\infty$ to ∞ (as a solitary wave has infinite period), leaving an averaged Lagrangian $\mathcal{L}$ which is a function of Z [40]. Variations of this averaged Lagrangian with respect to the nematicon parameters yield (modulation) equations determining its trajectory [40]. This Whitham modulation theory is a version of the applied mathematics method of multiple scales [41] optimized for slowly varying, nonlinear dispersive waves. However, the nematic equations (13) and (14) have no known general nematicon (solitary wave) solutions, but only isolated solitary wave solutions for fixed parameter values [42]. When there are no exact solutions on which to base modulation equations, variational approximations are useful and give accurate predictions [43]. In the present context, they yield results for nematicon refraction and scattering in excellent agreement with both numerical solutions [34, 44–47] and experimental results [35, 48, 49]. Variational methods usually require the use of a reasonable approximation to the unknown solitary wave profile. However, for the derivation of the momentum equations governing the trajectory of the nematicon this is not necessary and the profile can be left general, for reasons discussed below. We then assume that the nematicon solution has the form

$$u = a f_e(\rho_e) e^{i\sigma + iV(Y-\xi)} \quad \text{and} \quad \psi = \alpha f_d(\rho_d), \quad (17)$$

where

$$\rho_e = \frac{\sqrt{X^2+(Y-\xi)^2}}{w}, \quad \rho_d = \frac{\sqrt{X^2+(Y-\xi)^2}}{\beta}. \quad (18)$$

The nematicon f_e and director f_d profiles are not stated and are not needed to determine the nematicon trajectory. As the nematicon evolves due to the change in the medium, its amplitude a and width w oscillate and it refracts, so that its velocity V and position ξ evolve. It was found earlier [44, 45, 47] that the amplitude/width evolution of the soliton decouples from its trajectory evolution due to the highly nonlocal response [7]. The main effect of the nematicon amplitude/width oscillations is to cause it to shed dispersive radiation enabling it to reach a steady state. This radiation has momentum and so affects the nematicon trajectory, in turn. However, for a large nonlocality the shed radiation has low amplitude and is emitted on a long z scale [39, 44], so that the approach to a steady state is very slow. In fact, the high nonlocality gives rise to a very wide potential well around the evolving solitary wave, which essentially traps the radiation. As we are only interested in the nematicon trajectory, we can assume that its amplitude a and width w, as well as the amplitude α and width β of the molecular director distribution, are constant and consider that only the velocity V and position ξ depend on Z. Substituting the nematicon trial functions (17) into the Lagrangian (16) and averaging results in the averaged Lagrangian

$$\mathcal{L} = -2S_2\left(\sigma' - V\xi'\right)a^2w^2 - S_{22}a^2 - S_2\left[V^2 + 2V\gamma\Delta\left(\theta_0(0)+\theta_b(Z)\right)\right]a^2w^2 + 4\frac{\sin 2\left(\theta_0(0)+\theta_b(Z)\right)}{\sin 2\theta_0(0)}\alpha a^2 w^2 S_m - 4\nu S_{42}\alpha^2. \quad (19)$$

The integrals S_2, S_{22}, S_{42} and S_m appearing in the averaged Lagrangian are

$$S_2 = \int_0^\infty \zeta f_e^2(\zeta)\,d\zeta, \quad S_{22} = \int_0^\infty \zeta f_e'^2(\zeta)\,d\zeta,$$
$$S_{42} = \frac{1}{4}\int_0^\infty \zeta\left[\frac{d}{d\zeta}f_d(\zeta)\right]^2 d\zeta,$$
$$S_m = \int_0^\infty \zeta f_e^2(\zeta) f_d\left(\frac{w}{\beta}\zeta\right)d\zeta. \quad (20)$$

Taking variations of the averaged Lagrangian (19) with respect to the velocity V and position ξ results in the modulation equations

$$\frac{dV}{dZ} = 0, \quad (21)$$

$$\frac{d\xi}{dZ} = V + \gamma\Delta\left(\theta_0(0)+\theta_b(Z)\right). \quad (22)$$

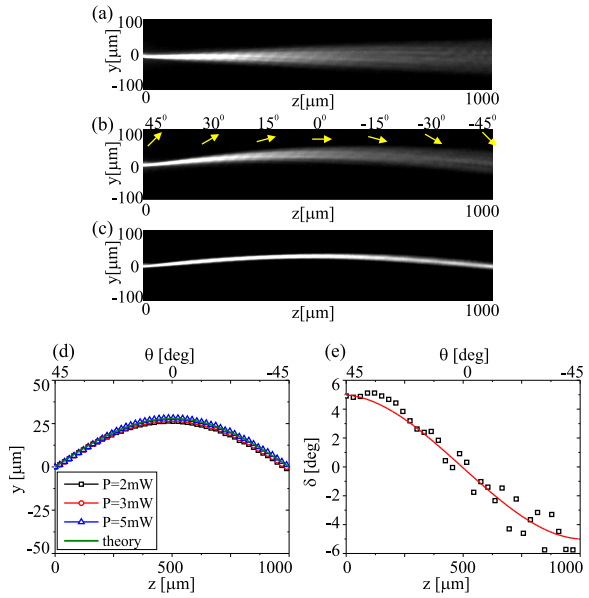

FIG. 3: (a–c) Photographs of nematicon evolution in the (y, z) plane of observation for (a) TM-like beam and TE-like beam with input power (b) $P = 1mW$ and (c) $P = 3mW$, respectively; the yellow arrows indicate the director orientation; (d) experimentally acquired (symbols) and theoretical (solid line) nematicon trajectories for various input powers; (e) computed (red line) and measured walk-off (black squares) versus propagation distance.

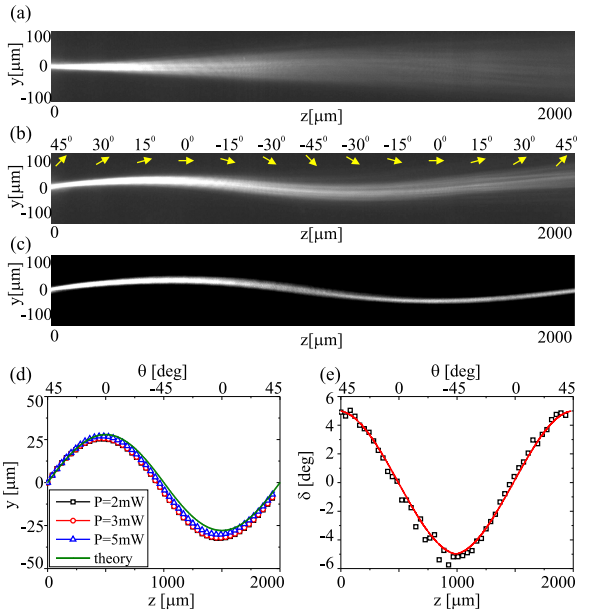

FIG. 4: (a–c) Images of nematicon evolution in the (y, z) plane for (a) TM-like and (b–c) TE-like beams of power (b) $P = 1mW$ and (c) $P = 3mW$, respectively; the yellow arrows indicate the director orientation; (d) experimentally acquired (symbols) and theoretical (solid line) nematicon trajectories for various input powers; (e) computed (red line) and measured (black squares) walk-off versus propagation distance.

These modulation equations are momentum equations for the nematicon trajectory. The nematicon velocity does not change and is fixed by its value at input, unlike nematicon refraction when the medium varies in the lateral (X, Y) directions [34, 35]. This is because the medium only varies in the longitudinal direction Z, which is a time-like variable for the NLS-type equation (13).

The director angle variation θ_b for the structure in Fig. 2(a) is linear in z (and Z). The imposed angle at $Z = 0$ is $\theta_b = 0$. We set the angle at the end of the cell as θ_r at the non-dimensional distance $Z = L_n$. In this case

$$\theta_b(Z) = mZ, \quad m = \frac{\theta_r - \theta_0(0)}{L_n}. \tag{23}$$

The position equation (22) then has the solution

$$\xi = \xi_0 + VZ - \frac{\gamma}{2m} \ln \frac{\Delta\epsilon + 2n_\perp^2 + \Delta\epsilon \cos 2\left(\theta_0(0) + mZ\right)}{\Delta\epsilon + 2n_\perp^2 + \Delta\epsilon \cos 2\theta_0(0)} \tag{24}$$

for the nematicon trajectory, where ξ_0 is the non-dimensional input beam position. The solution (24) also applies in the second half of the structure in Fig. 2(b) for which the imposed background angle varies from $-\pi/4$ to $\pi/4$ by setting $\theta_0(0) = -\pi/4$ and $\theta_r = \pi/4$. However, as $\cos x$ is antisymmetric about $x = \pi/2$, the solution (24) also applies to the whole structure in Fig. 2(b) as is.

IV. EXPERIMENTAL AND NUMERICAL RESULTS FROM NON-UNIFORM SAMPLES

We firstly investigated a sample with the structure illustrated in Fig. 2(a), acquiring the nematicon path for a director orientation changing from 45^0 at $z = 0$ to -45^0 at $z = 1000\mu$m. Fig. 3 shows the experimentally acquired beam evolution in the principal plane (y, z). For an ordinary wave (TM-like) input beam, the structure behaves as a uniform sample with an ordinary refractive index, leading to linear diffraction of the beam (Fig. 3(a)). For an extraordinary wave (TE-like) beam, the non-uniform orientation has a significant impact on the trajectory. Fig. 3(b) shows the acquired image of a TE beam at low power (linear diffraction), while Fig. 3(c) is the corresponding case at high power, above $2mW$, such that a nematicon was generated. The nematicon path follows the change in orientation, resulting in the bent trajectory displayed in Fig. 3(d). Fig. 3(e) graphs the comparison between the calculated (red line) and the measured (black squares) walk-off versus propagation distance, showing excellent agreement. In the weakly nonlinear regime of interest here the beam walk-off remains essentially determined by the background orientation $\theta_0(z)$.

Next we examined the role of walk-off on a nematicon path for the case of the director orientation changing from 45^0 at $z = 0$ to -45^0 at $z = 1000\mu$m and back to 45^0 at $z = 2000\mu$m, as in Fig. 2(b). Fig. 4 shows photographs of the acquired beam evolution. As in the previous case

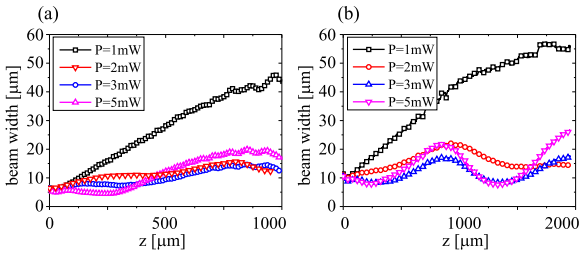

FIG. 5: Measured beam width versus propagation distance for various input powers in the two investigated geometries (Fig. 2(a) and Fig. 2(b)): (a) the orientation changes from 45^0 to -45^0 over $z = 1000\mu$m; (b) the orientation changes from 45^0 and back to 45^0 over $z = 2000\mu$m.

(Fig. 3(a)) an ordinary wave (TM-like) beam diffracts and evolves essentially along $\mathbf{k} \parallel \hat{\mathbf{z}}$. (Fig. 4(a)). Panels 4(b–c) are images of a TE-like beam at low power (linear diffraction) and at high excitation with nematicon formation, respectively. At powers near or slightly above $2mW$, the input beam becomes self-confined with its walk-off determined by the change in orientation, resulting in a doubly bent trajectory (Fig. 4(d)). Fig. 4(e) compares the calculated (red line) and measured (black squares) walk-off versus propagation distance for the high power case. Once again, the agreement is remarkably good.

It can be seen on comparing the theoretical and experimental trajectories of Figures 3(d) and 4(d) that the difference between them grows with propagation distance. This is due to the accumulation of errors in the asymptotic analysis leading to the momentum equations (21) and (22) as z increases. These errors are due to (i) the neglect of the optical contribution ψ in the walkoff Δ in the electric field equation (13), (ii) the linearisation of the full nematic equations (3) and (4) assuming that the optical reorientation ψ is small and (iii) the neglect of scattering losses.

Noteworthy, even though the background reorientation $\theta_0(z)$ goes through 0^0 where no nonlinear response is expected below the Freedericksz transition, self-confinement and the nematicon survive without significant change owing to the abiabatic character of the modulation. Such robustness of a solitary wave solution across non-uniform regions— including linear regions— is supported by the large nonlocality of the medium, even along the propagation coordinate (see also Ref. [50]).

Finally, Fig. 5 compares the measured e-wave beam widths versus propagation distance in both the investigated geometries and for various input beam powers. These plots confirm the breathing character of reorientational spatial solitons in NLC [51].

V. CONCLUSIONS

We have demonstrated solitary wave bending and double bending in longitudinally modulated nematic liquid crystals with an optic axis orientation linearly varying along the propagation distance. In such a configuration the curved trajectory is solely due to changes in walk-off without refraction effects, allowing for an excellent match between a simplified model and the experimental results. This investigation, singling out the role of birefringence against the combined effects of birefringence and refraction, is of relevance in the design and realization of reorientational structures utilizing both transverse and longitudinal modulations of the director orientation, paving the way for the engineering of desired solitary wave paths, either in the dynamic limit or for permanent guided-wave photonics, based on beam-induced material moulding through nonlinear sculpting [14].

Acknowledgements

U. A. L. and M. K. thank the National Centre for Research and Development grant agreement LIDER/018/309/L-5/13/NCBR/2014. G. A. acknowledges support from the Academy of Finland through the FiDiPro grant no. 282858. We are indebted to M. Swiniarski (Faculty of Physics, Warsaw University of Technology) for helping with sample preparation using electron-beam lithography.

[1] I. Khoo, *Liquid Crystals: Physical Properties and Nonlinear Optical Phenomena*, John Wiley & Sons (2007).
[2] L. Vicari, *Optical Applications of Liquid Crystals*, CRC Press (2016).
[3] D. Yang, *Fundamentals of Liquid Crystal Devices*, John Wiley & Sons (2014).
[4] N. V. Kamanina, *Features of liquid crystal display materials and processes*, InTech (2011).
[5] G. Assanto and M. Karpierz, Liq. Cryst. **36**, 1161 (2009).
[6] G. Assanto, editor, *Nematicons*, John Wiley & Sons (2012).
[7] M. Peccianti and G. Assanto, Nematicons, Phys. Rep. **516**, 147–208 (2012).
[8] M. Peccianti, A. Fratalocchi, and G. Assanto, Transverse dynamics of nematicons, Opt. Express **12**, 6524–6529 (2004).
[9] M. Peccianti, C. Conti, G. Assanto, A. De Luca, and C. Umeton, Routing of anisotropic spatial solitons and modulational instability in liquid crystals, Nature **432**, 733–737 (2004).
[10] M. Kwasny, U. A. Laudyn, F. Sala, A. Alberucci, M. A. Karpierz and G. Assanto, Self-guided beams in low-birefringence nematic liquid crystals, Phys. Rev. A **86**, 013824 (2012).
[11] M. Peccianti and G. Assanto, Signal readdressing by steering of spatial solitons in bulk nematic liquid crys-

tals, Opt. Lett. **26**, 1690–1692 (2001).
[12] G. Assanto and M. Peccianti, Spatial solitons in nematic liquid crystals, IEEE J. Quantum Electron. **39**, 13–21 (2003).
[13] A. Piccardi, A. Alberucci, U. Bortolozzo, S. Residori, G. Assanto, Readdressable interconnects with spatial soliton waveguides in liquid crystal light valves, IEEE Photon. Techn. Lett. **22**, 694–696 (2010).
[14] N. Karimi, M. Virkki, A. Alberucci, O. Buchnev, M. Kauranen, A. Priimagi, and G. Assanto, Molding optical waveguides with nematicons, Adv. Opt. Mat. Commun. **5** , 1700199 (2017).
[15] A. Piccardi, M. Peccianti, G. Assanto, A. Dyadyusha and M. Kaczmarek, Voltage-driven in-plane steering of nematicons, Appl. Phys. Lett. **94**, 091106 (2009).
[16] Y. V. Izdebskaya, Routing of spatial solitons by interaction with rod microelectrodes, Opt. Lett. **96**, 061105 (2010).
[17] R. Barboza, A. Alberucci, and G. Assanto, Large electro-optic beam steering with nematicons, Opt. Lett. **36**, 2611–2613 (2011).
[18] J. Beeckman, K. Neyts, M. Haelterman, Patterned electrode steering of nematicons, J. Opt. A Pure Appl. Opt. **8**, 214 (2006)
[19] M. Peccianti, A. Dyadyusha, M. Kaczmarek, and G. Assanto, Tunable refraction and reflection of self-confined light beams, Nat. Phys. **2**, 737–42 (2006).
[20] M. Peccianti, G. Assanto, A. Dyadyusha and M. Kaczmarek, Non-Specular Total Internal Reflection of spatial solitons at the interface between highly birefringent media, Phys. Rev. Lett. **98**, 113902 (2007).
[21] M. Peccianti and G. Assanto, Nematicons across interfaces: anomalous refraction and reflection of solitons in liquid crystals, Opt. Express **15**, 8021–8028 (2007).
[22] A. Piccardi, G. Assanto, L. Lucchetti and F. Simoni, All-optical steering of soliton waveguides in dye-doped liquid crystals, Appl. Phys. Lett. **93**, 171104 (2008).
[23] A. Alberucci, M. Peccianti, G. Assanto, Nonlinear bouncing of nonlocal spatial solitons at the boundaries, Opt. Lett. **32**, 2795–2797 (2007).
[24] A. Piccardi, A. Alberucci, and G. Assanto, Power-dependent nematicon steering via walk-off, J. Opt. Soc. Am. B **27**, 2398–2404 (2010)
[25] A. Piccardi, A. Alberucci, and G. Assanto, Soliton self-deflection via power-dependent walk-off, Appl. Phys. Lett. **96**, 061105 (2010).
[26] A. Piccardi, A. Alberucci, and G. Assanto, Self-turning self-confined light beams in guest-host media, Phys. Rev. Lett. **104**, 213904 (2010).
[27] A. Alberucci, A. Piccardi, N. Kravets, O. Buchnev, and G. Assanto, Soliton enhancement of spontaneous symmetry breaking, Optica **2**, 783–789 (2015).
[28] U. A. Laudyn and M. A. Karpierz, Nematicons deflection through interaction with disclination lines in chiral nematic liquid crystals, Appl. Phys. Lett. **103**, 221104 (2013).
[29] U. A. Laudyn, M. Kwasny, F. A. Sala, M. A. Karpierz, All optical and electro-optical switches based on the interaction with disclination lines in chiral nmatic liquid crystals, J. Opt. **18**, 054011 (2016).
[30] Y. Izdebskaya, V. Shvedov, G. Assanto, and W. Krolikowski, Magnetic routing of light-induced waveguides, Nat. Comm. **8**, 14452 (2017).
[31] V. Shvedov, Y. Izdebskaya, Y. Sheng, and W. Krolikowski, Magnetically controlled negative refraction of solitons in liquid crystals, Appl. Phys. Lett. **110**, 091107 (2017).
[32] S. Slussarenko, A. Alberucci, C.-P. Jisha, P. Piccirillo. E. Santamato, G. Assanto and L. Marrucci, Guiding light via geometric phases, Nat. Photon. **10**, 571–575 (2016).
[33] A. Alberucci, C. P. Jisha, L. Marrucci and G. Assanto, Electromagnetic waves in inhomogeneously anisotropic dielectrics: confinement through polarization evolution, ACS Photon. **3**, 2249–2254 (2016.)
[34] F. A. Sala, N. F. Smyth, U. A. Laudyn, M. A. Karpierz, A. A. Minzoni and G. Assanto, Bending reorientational solitons with modulated alignment, J. Opt. Soc. Am. B **34**, 2459–2466 (2017).
[35] U. A. Laudyn, M. Kwaśny, F. A. Sala, M. A. Karpierz, N. F. Smyth and G. Assanto, Curved optical solitons subject to transverse acceleration in reorientational soft matter, Sci. Rep. **7**, 12385 (2017).
[36] R. Dabrowski, New liquid crystalline materials for photonic applications, Mol. Cryst. Liq. Cryst. **421**, 1–21 (2004).
[37] T. Kagajyo, K. Fujibayashi, T. Shimamura, H. Okada, H. Onnogawa, Alignment of nematic liquid crystal molecules using nanometer-sized ultrafine patterns by electron beam lithography, Jpn. J. Appl. Phys. **44**, 578–581 (2005).
[38] A. Alberucci, A. Piccardi, M. Peccianti, M. Kaczmarek and G. Assanto, Propagation of spatial optical solitons in a dielectric with adjustable nonlinearity, Phys. Rev. A **82**, 023806 (2010).
[39] A.A. Minzoni, N.F. Smyth and A.L. Worthy, Modulation solutions for nematicon propagation in non-local liquid crystals, J. Opt. Soc. Am. B **24**, 1549–1556 (2007).
[40] G.B. Whitham, *Linear and Nonlinear Waves,* J. Wiley and Sons, New York (1974).
[41] J.D. Cole and J. Kevorkian, *Perturbation Methods in Applied Mathematics,* Springer-Verlag, New York (1981).
[42] J.M.L. MacNeil, N.F. Smyth and G. Assanto, Exact and approximate solutions for solitary waves in nematic liquid crystals, Physica D **284**, 1–15 (2014).
[43] B. Malomed, Variational methods in nonlinear fiber optics and related fields, Prog. Opt. **43**, 71–193 (2002).
[44] B. D. Skuse and N. F. Smyth, Interaction of two colour solitary waves in a liquid crystal in the nonlocal regime, Phys. Rev. A **79**, 063806 (2009).
[45] A. Alberucci, G. Assanto, A. A. Minzoni and N. F. Smyth, Scattering of reorientational optical solitary waves at dielectric perturbations, Phys. Rev. A **85**, 013804 (2012).
[46] N. F. Smyth and W. Xia, Refraction and instability of optical vortices at an interface in a liquid crystal, J. Phys. B: Atom. Molec. Opt. Phys. **45**, 165403 (2012).
[47] G. Assanto, A. A. Minzoni, N. F. Smyth and A. L. Worthy, Refraction of nonlinear beams by localised refractive index changes in nematic liquid crystals, Phys. Rev. A **82**, 053843 (2010).
[48] G. Assanto, A. A. Minzoni, M. Peccianti and N. F. Smyth, Optical solitary waves escaping a wide trapping potential in nematic liquid crystals: modulation theory, Phys. Rev. A **79**, 033837 (2009).
[49] G. Assanto, N. F. Smyth and W. Xia, Modulation analysis of nonlinear beam refraction at an interface in liquid crystals, Phys. Rev. A **84**, 033818 (2011).
[50] A. Alberucci, M. Peccianti, G. Assanto, G. Coschignano,

A. De Luca and C. Umeton, Self-healing generation of spatial solitons in liquid crystals, Opt. Lett. **30**, 1381–1383 (2005).

[51] C. Conti, M. Peccianti and G. Assanto, Observation of optical spatial solitons in a highly nonlocal medium, Phys. Rev. Lett. **92**, 113902 (2004).